



The improvement of modelled wind and wave fields with increasing resolution

Luigi Cavaleri*, Luciana Bertotti

Institute of Marine Sciences (ISMAR), S.Polo 1364, 30125 Venice, Italy

Received 2 February 2005; accepted 28 July 2005

Available online 17 November 2005

Abstract

We have simulated a number of periods using different resolutions of the ECMWF meteorological model. Then we have explored how the quality of the surface wind and wave model results varies with the resolution. The comparisons have been done in the oceans and in the Mediterranean Sea, using measured data from buoys and satellite.

At the highest resolution we have used, T799 or 25 km, the biases in the oceans reduce to very small values of the order of a few percent. In enclosed seas, represented in this case by the Mediterranean, the errors decrease with increasing resolution, but a substantial underestimate still remains.

The maximum values of both the wind speeds and the wave heights increase with resolution. However, the suggestion is that even T799 fails to model properly the highest peaks of the storms, a fact possibly due to the inaccurate description of physics in these extreme events. This seems particularly true in the case of a cyclone in the Bay of Bengal.

© 2005 Elsevier Ltd. All rights reserved.

Keywords: Wind; Waves; Meteorological models; Numerical models; Wave modelling; Resolution

1. Introduction

In a previous paper, (Cavaleri and Bertotti, 2003, henceforth referred to as CB) we reported on a series of numerical experiments aimed at exploring how the results from a meteorological model and the associated wave model depend on the resolution.

* Corresponding author. Fax: +39 041 2602340.

E-mail address: luigi.cavaleri@ismar.cnr.it (L. Cavaleri).

In particular, we analysed the model behaviour both in the oceans and in the Mediterranean Sea, the latter being considered as representative of enclosed basins. Following further experiments also done with different and higher resolutions, this paper extends the previous results, focusing on surface wind speed and on wave height.

The structure of the experiments is described in Section 2. In Section 3, we report the results on the oceans; in Section 4, the results for the Mediterranean Sea. In Section 5, we discuss the ability to model the essential features of a cyclone. The discussion and conclusions are in the final Sections 6 and 7.

2. The organisation of the tests

Similarly to CB, for our tests we have selected seven different periods, each lasting between 3 and 12 days for an overall 46 days, and simulated them using the global meteorological model presently operational at the European Centre for Medium-Range Weather Forecasts (ECMWF, Reading, UK; see [Simmons, 1991](#), and [Simmons et al., 1995](#)). The model is fully coupled with the WAM wave model ([Komen et al., 1994](#)), thereby providing at the same time series of global wind and wave conditions on the oceans. In the enclosed seas the resolution of the global WAM model, 0.5° , is not sufficient for a proper description of the local details. Hence, for the Mediterranean Sea we have carried out separate wave hindcasts with 0.25° resolution, using as input the already evaluated surface wind fields.

The seven periods are listed in [Table 1](#). They have been chosen to correspond with some relevant events in the Mediterranean Sea, and are therefore concentrated in the north hemisphere winter. On the other hand, the variety of events present on the global scale ensures that storms were present also on the oceans. On top of these, to check the model capability to deal with very strong spatial gradients, we have selected a cyclone in the Bay of Bengal.

All the above events have been modelled with six different resolutions of the meteorological model, listed in [Table 2](#). The ECMWF model is spectral, the characterisation, e.g. T511, providing the truncation level T of the Fourier time series used to describe the fields. Each simulation, for given period and resolution, was modelled with a sequence of 72 h forecasts, as shown in [Fig. 1](#). The starting dates of each forecast were chosen 48 h apart. From each 72 h experiment, we have used the data from the last

Table 1
Periods chosen for the experiments

1	9–12 Jan 1987
2	31 Dec 1992–12 Jan 1993
3	4–12 Feb 1994
4	8–17 Jan 1995
5	18–21 Mar 1995
6	26 Mar–1 Apr 1995
7	27 Dec 2000–1 Jan 2001
8	14–20 May 1997

Table 2

Truncation levels T considered for the meteorological model, and corresponding spatial resolutions R in kilometres

T	106	213	319	511	639	799
R (km)	188	94	63	39	31	25

48 h to allow the model to develop during the first day the characteristics of the fields corresponding to its resolution. Combined with also the first day of the first experiment, this (Fig. 1) gave a continuous sequence of wind and wave fields at 6 h intervals. For each experiment the initial conditions were given by the analysis available at ECMWF. On the whole the procedure produced 184×6 fields, plus the ones for the cyclone, available for later analysis.

3. Results for the oceans

Our analysis has proceeded in two directions. First, we have intercompared the results obtained with the different resolutions of the meteorological model. This has been done separately for wind speed U_{10} and wave height H_s . Then the comparison has been done against the measured data. For the latter ones, we have made use of 36 buoys present in the Northern Atlantic and Northern Pacific oceans, available from the web. Their wide geographical distribution makes them well representative of the average behaviour of the models (with differences to be discussed later). The data were selected in correspondence of the times at which the experiment data were available (00, 06, 12, 18 UT).

For each pair of resolutions, e.g. T511 and T639, we have considered the corresponding co-located, e.g. wind speed, values, in space and time, and checked by best-fitting their scatter distribution how much U_{10} and H_s vary with increasing resolution. An example is given in Fig. 2, where the T639 surface wind speeds over the sea are compared with the T511 ones. The overall results are conveniently summarised in Fig. 3 for U_{10} and in Fig. 4 for H_s , where the T106 results have been taken as unitary reference value. Note that in all the four panels of the two figures the vertical scale varies between 1 and 1.3 to better compare the different rates of improvement. The results are provided separately for the northern hemisphere (NH), the tropics (TP, $\pm 30^\circ$), the southern hemisphere (SH), and the

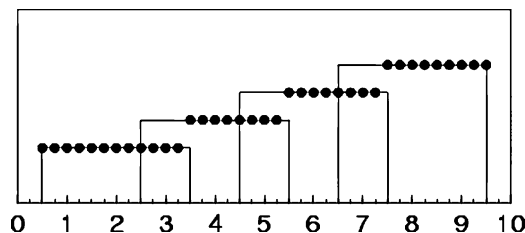


Fig. 1. Scheme of the different experiments for a given period, and selection of the fields, at 6 h intervals, for later analysis (after Cavaleri and Bertotti, 2003).

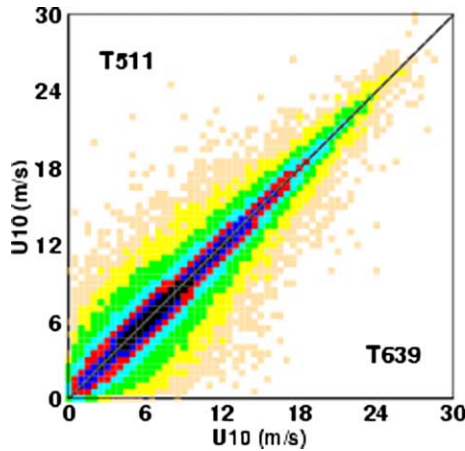


Fig. 2. Scatter diagram between the wind speeds from the T511 and T639 runs.

Mediterranean Sea (Med). In this section, we discuss those for the oceans, i.e. NH, TP, SH (respectively, N-HEM, TROPI, S-HEM in the figures).

Considering first the wind speed (left panel of Fig. 3), we see that in all the three zones the results approach a limiting value. The increase in the NH is slightly stronger, probably because of the local winter conditions. Indeed, considering also the quality of the present ECMWF operational results with T511 (e.g. Simmons and Hollingsworth, 2002, and Bidlot et al., 2002), this suggests that a further increase of resolution will move them very close to the measured ones. This is confirmed by the wind bias with respect to the buoy data reported in Table 3 (first row).

Given the direct dependence of H_s on U_{10} , a similar increase is expected also for H_s (left panel of Fig. 4). However, here the comparison against the buoy data is less satisfactory

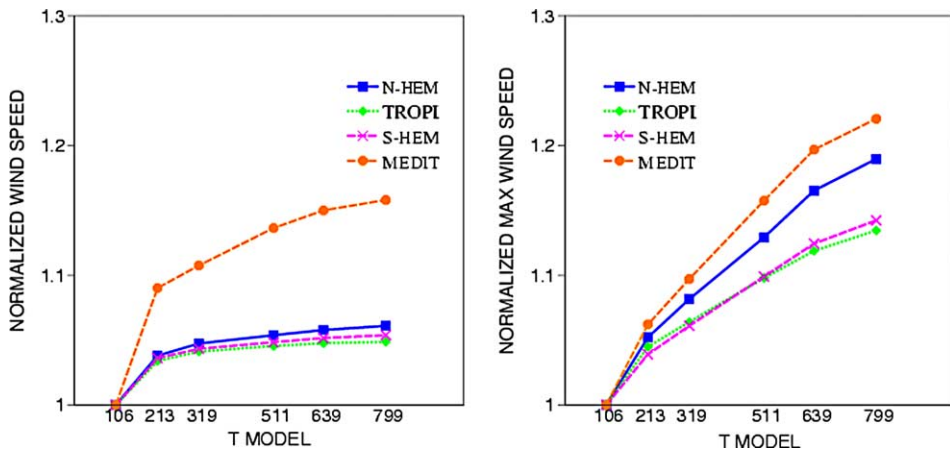


Fig. 3. Left panel: relative increase of the wind speeds with the resolution of the meteorological model. Right panel: as the left diagram, but for maximum wind speeds.

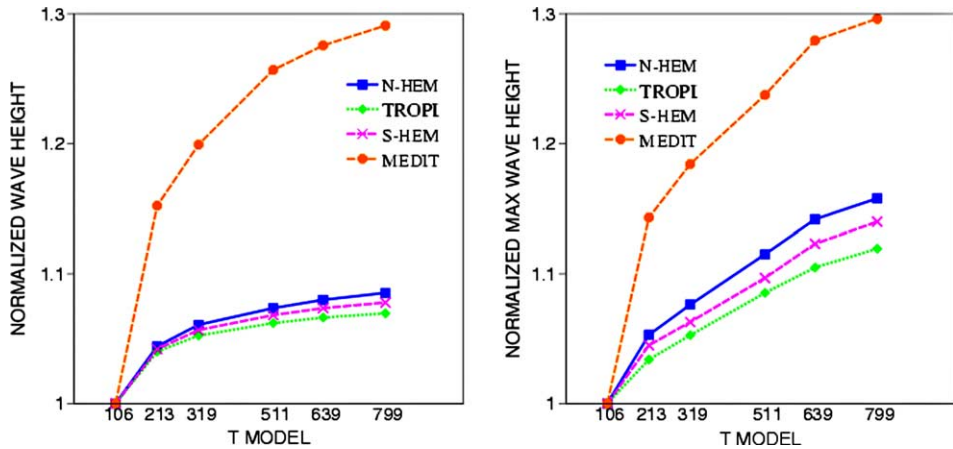


Fig. 4. Left panel: relative increase of the wave heights with the resolution of the meteorological model. Right panel: as the left diagram, but for maximum wave heights.

(Table 3, third row), because there is a definite tendency towards a 20 cm negative bias. A possible explanation will be given in the discussion in Section 6.

The inspection of the scatter values SI in Table 3, defined as the ratio between the root mean square error and the average value of the reference variable, for all the above cases tells a rather different story. Briefly summarised, the indication is that, when increasing the resolution R of the meteorological model, there is no improvement, i.e. no decrease of SI, either for wind as for waves. In our experiment, the scatter of the results with respect to the measured data is due to four reasons: (a) small errors in the analysis, that rapidly increase with the extent of the forecast, (b) incorrect physics and numerics of the models, (c) insufficient resolution, (d) the intrinsic variability of the atmosphere. The role of (a) + (b) + (c) vs (d) can be quantified by analysing how the scatter varies with the extent of the forecast. If the basic reason for it lies in the incorrect analysis and/or in the model, we must expect the scatter to grow with time. Conversely, a constant R or large values since the start of the experiments will point to the variability of the atmosphere as the basic reason for it. We have analysed our results in 12 h forecast sections, i.e. analysing in the first section the analysis, in the second one all the +6 and +12 h forecasts, and so on until +66 and +72 h. The comparison with measured data has been repeated for each section

Table 3
Statistics (bias and scatter index SI) for wind speed (m/s) and wave height (m) model results against 36 widely distributed ocean buoy data

		T106	T213	T319	T511	T639	T799
Wind	Bias	-0.16	-0.08	-0.03	-0.01	0.01	0.01
	SI	0.29	0.29	0.30	0.30	0.30	0.30
Waves	Bias	-0.28	-0.24	-0.23	-0.22	-0.21	-0.20
	SI	0.25	0.25	0.25	0.25	0.25	0.25

Different resolutions of the meteorological model have been used (Table 2).

and each resolution. All the results consistently indicate, for each resolution, analysis SI values close to 0.20, progressively increasing with the extent of the forecast, up to 0.35 for U_{10} and 0.30 for H_s . The values reported in Table 3 turn out to be averages along the different forecasts periods. Therefore, the suggestion is that there is an initial scatter, associated to errors in the analysis and to the natural variability of the fields. Note that the SI values for wind are always larger than the ones for waves. While this is partly due to the longer memory of the wave fields, an integral product of the driving wind fields, it also supports the hypothesis of the atmospheric variability as a basic reason for the scatter (Abdalla and Cavaleri, 2002). Should SI be due only to substantial errors in the meteorological pattern, this would also be reflected in the wave fields.

We now focus our attention on the maximum values. This is still an open problem because the peak values in a storm are frequently underestimated. There are doubts about the physics of the processes in these conditions and on the capability of the model to reproduce them. Powell et al. (2003) give a good summary of the situation. However, there are also obvious reasons in the numerics of the models. One is the resolution, the other one is the horizontal diffusion introduced for numerical stability (Cavaleri et al., 1997). Both these tend to smooth the fields and to decrease the peak values, particularly in areas characterised by strong spatial horizontal gradients. We have explored the implications by comparing the 46 days (184 fields) of simulation available for each resolution (Section 2). One limitation of this analysis is the lack of comparison with measured data. As the maxima are isolated in space and time, only in a few rare cases is the ground truth available at the right time and position.

For each resolution and for each one of the available 184 fields, we have extracted the maximum value, for wind speed and wave height. Then, similarly to what done for the overall wind speeds, we have determined the best-fit slope for each pair of resolutions (T106 vs T213, T213 vs T319, etc). Normalised with respect to T106, the results are shown in the right panels of Figs. 3 and 4 (the Mediterranean data will be discussed in Section 4). We see that, in contrast to the overall quantities in the left panels, the maxima do not show a tendency toward an asymptotic value. This suggests that even at T799 we are not yet able to resolve properly the peaks of the distribution. This differences are stronger for the wind speeds than for the wave heights. The latter depend on the overall driving wind fields, and therefore, they are less sensitive to an underestimate of the wind peaks.

4. Results for the Mediterranean Sea

Similarly to the oceans, first we analyse how the model results vary with resolution, then we provide a quantitative estimate of their performance.

From the left panels of Figs. 3 and 4, we recognise at once the dramatic increase of both the wind speeds and the wave heights with increasing resolution, particularly evident in the two figures when compared to the corresponding ocean results. In the upper R values, there is some indication of a tendency towards an asymptotic behaviour for U_{10} (left panel of Fig. 3). However, the corresponding diagram for H_s (left panel of Fig. 4) shows a substantial increase of the wave height also when passing from T639 to T799. This

suggests that also the highest resolution does not succeed in modelling properly the wind, hence the wave, fields in the Mediterranean and, more in general, in the enclosed basins. As expected, the gain for H_s is larger than for U_{10} . In areas without or with limited swell, as it is the case in the enclosed seas, the H_s dependence on U_{10} can be expressed as $H_s \propto U_{10}^\beta$, with β varying from 1 to 2 from fetch limited to open sea well developed conditions. In the intermediate conditions of the Mediterranean Sea, assuming $\beta = 1.5$, we have $\Delta H_s \% \approx 1.5 \Delta U_{10} \%$. Indeed, this is what we find approximately in the statistics shown above.

A quantification of the actual performance of the model has been obtained by a long-term comparison of the operational T511 results against the Topex data. The period considered goes from December 2000 to June 2002. For each altimeter datum, at about seven kilometre and 1 s intervals, the model results, available at six h intervals, have been linearly interpolated in space and time to obtain the pairs of co-located values. All the available pairs have been distributed to the closest grid point, at 0.5° intervals. Best-fitting a line to the set of pairs at each point provided an estimate of the local average ratio between model and altimeter data. This has been done separately for wind speed and wave height.

The overall results for the Mediterranean Sea are given in Fig. 5, showing the distribution of the average ratio between model and Topex Altimeter wind speeds. We recognise at once the substantial underestimate by the model. The distribution has a well-defined pattern. While values close to unity (100 in the figure) are found close to the African coast, the whole northern part of the basin is characterised by much lower values, down to 60 or 70 (40–30% underestimate, respectively) in the more enclosed parts like the Aegean Sea and the Ligurian and Adriatic seas (Fig. 5), the two upper basins, respectively, to the left and right of Italy. The results for waves follow accordingly.

These results are confirmed by the biases with respect to Topex data shown in Table 4 for each resolution and referred to the experiments periods (Table 1). We see that even at the highest resolution, T799, the wind speed has a bias of 0.21 m/s, about 4% of the overall average absolute value 5 m/s. While this percentage seems small enough, the distribution

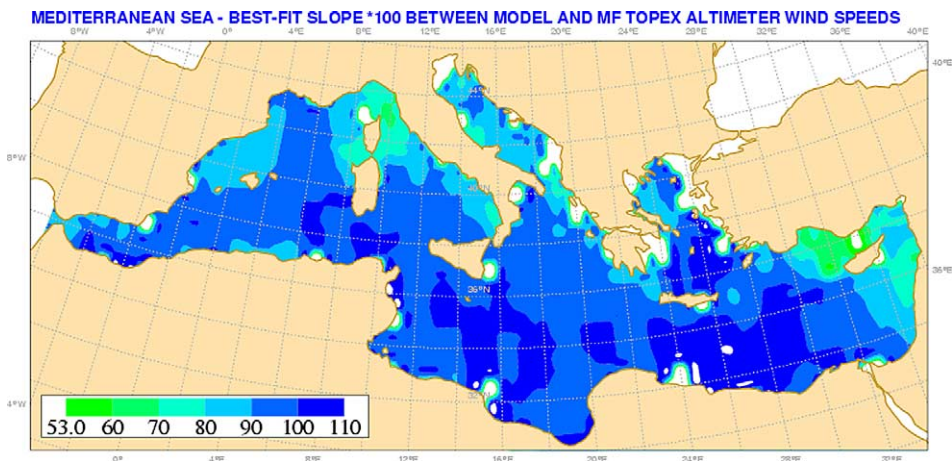


Fig. 5. Slope ($\times 100$) of the best-fit between model and Topex measured wind speeds in the Mediterranean Sea.

Table 4

Bias and scatter index SI for wind speed (m/s) and wave height (m) model results against Topex data in the Mediterranean Sea

		T106	T213	T319	T511	T639	T799
Wind	Bias	-0.83	-0.34	-0.31	-0.27	-0.24	-0.21
	SI	0.31	0.32	0.32	0.32	0.31	0.31
Waves	Bias	-0.64	-0.48	-0.45	-0.42	-0.37	-0.25
	SI	0.38	0.36	0.36	0.36	0.35	0.35

Different resolutions of the meteorological model have been used (Table 2).

in Fig. 5 suggests that most of the underestimate is concentrated in the northern part of the basin. Indeed, this is what we find exploring the geographical distribution of the experiments vs Topex comparison. As expected, the wave results follow a similar trend.

The values of the scatter index for wind speed are only slightly larger than in the oceans, a characteristic we consider associated to the effects of the orography and to the limited dimensions of the sub-basins. This is also manifest in the large scatter for H_s , because of the more ‘local’ generation by wind with respect to the scales of the oceans, often dominated by swell. A similar argument is derived from the increase of the maximum values with resolution, in the right panel of Fig. 3 (wind speed) and of Fig. 4 (wave height). In face of comparable increases of maximum U_{10} in the Mediterranean and in the oceans, the maximum H_s grow much more in the smaller basin, pointing to a more direct dependence on the local winds.

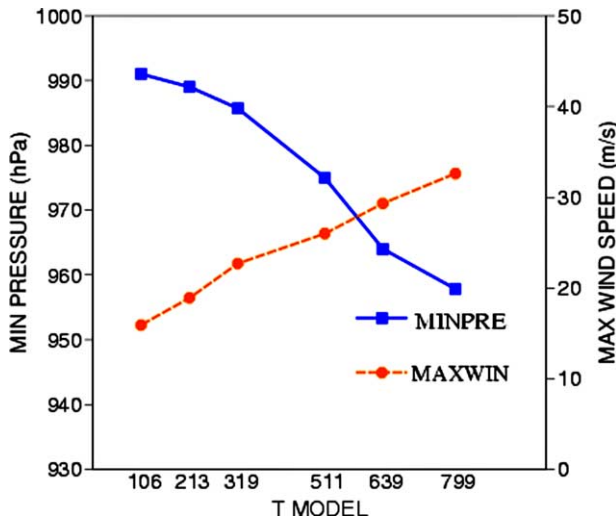


Fig. 6. Minimum pressure and maximum wind speed at the peak of a cyclone in the Bay of Bengal, according to different resolutions of the meteorological model. The minimum (p) and maximum (U_{10}) of the scales correspond to the reported extreme values.

5. A tropical cyclone

As an extreme example, we have analysed a tropical cyclone in the Bay of Bengal. Given the very large spatial gradients present in this kind of storm, it can be anticipated that even the maximum resolution, T799, corresponding to about 25 km, is not sufficient to represent properly the fields. Nevertheless, it is of interest to see how the results vary with the higher resolutions we have used.

We have hindcast the storm from May 14 to 20, 1997, from its early beginning, along its northwards path, until its landfall on the 20th. The peak was reached on May 19, with reported wind speeds up to 50 m/s and atmospheric surface pressure as low as 930 hPa (official report from the ECMWF archive). The hindcast has been done with the technique described in Section 2. Because of the sensitivity to the initial conditions, derived from T213, the global model operational at the time, we have used only 48-h forecasts, considering for our analysis the +24/+48 h sections.

First, we focus on the peak conditions, and we explore how the results change with the resolution R . Fig. 6 shows how the minimum pressure p and maximum wind speed U_{max} vary with R . As expected, increasing R leads to a steady increase of the strength of

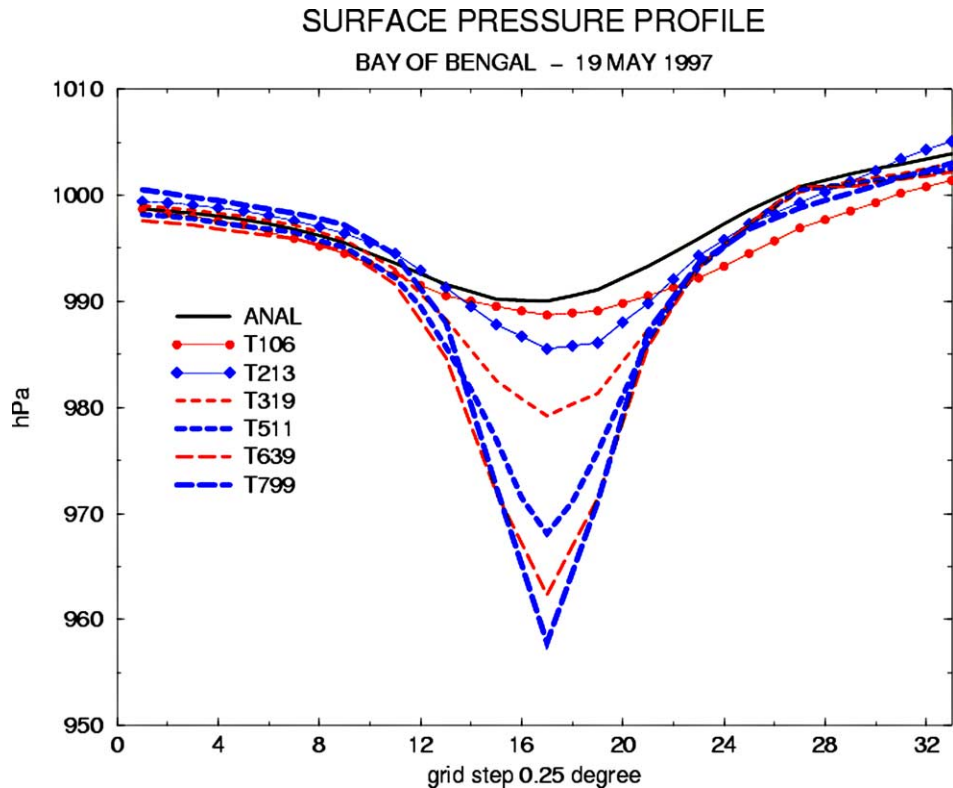


Fig. 7. Pressure distributions across a west-to-east section in a cyclone in the Bay of Bengal, according to different resolutions of the meteorological model.

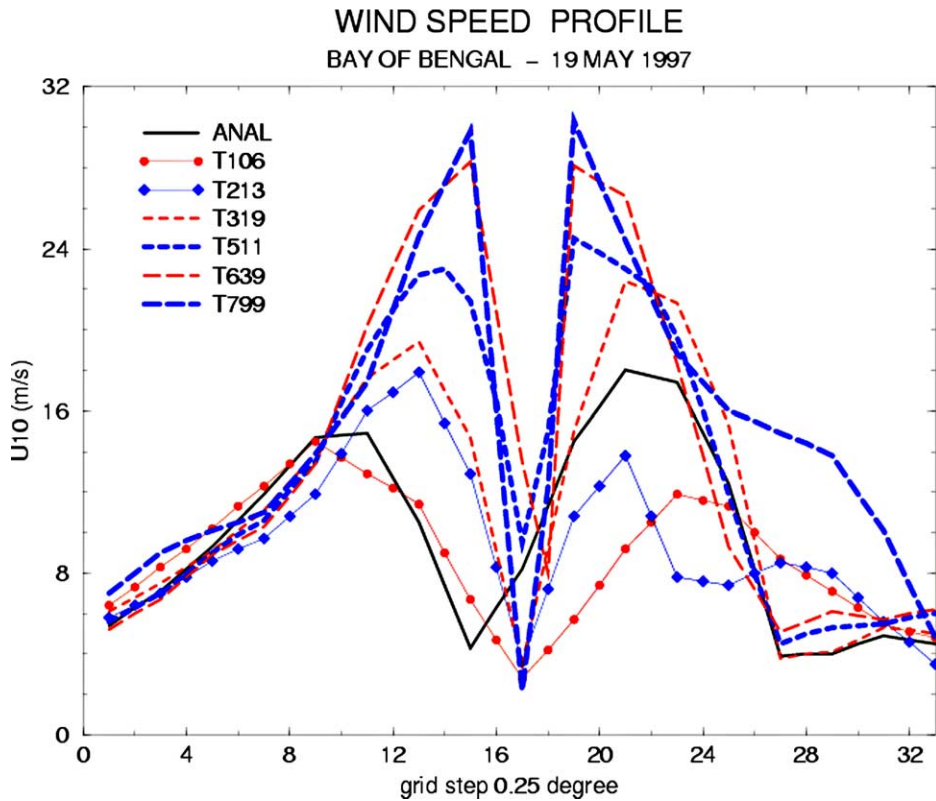


Fig. 8. Wind speed distributions along the same section of Fig. 7.

the storm. However, no asymptotic behaviour is evident, and even T799 fails to approach the extreme values reported during the cyclone life, corresponding to the lowest (p , left) and highest (U_{10} , right) values of the scales.

A more detailed view of the structure of the cyclone is obtained analysing how p and U_{10} vary along a west-to-east section across the eye of the cyclone. This is shown, respectively, in Figs. 7 and 8. Looking first at the p diagram, we recognise the expected reduced dimensions of the strongest part of the storm with increasing resolution, and the deepening at its centre. However, there is no evident real progress from T639 to T799, notwithstanding the minima are well off the 930 hPa reported value. The poor performance of the analysis (operational model) is noteworthy, much worse than the hindcast with the same resolution (T213). This points to the role of data assimilation and the limited resolution of its inner cycle in shaping areas with very strong spatial gradients.

In Fig. 8, showing the wind speed distributions, the structure of the cyclone is evident, with the minimum value of U_{10} at the eye position. T799 does indeed provide the lowest value, about 2 m/s, which is realistic. While the higher R 's provide also the higher wind speeds, we were surprised to find only a limited enhancement in this range, the peaks being still well below the reported 50 m/s. Also, the structure lacks the typical asymmetry of

a cyclone, with higher wind speeds on its right flank (with respect to its motion, if in the northern hemisphere, hence counterclockwise rotation). This asymmetry is recognised in the analysis, possibly a feature introduced by the data assimilation.

6. Discussion

The technique we have used, a sequence of relatively short forecasts, can only be partly indicative of the performance of a corresponding operational model. However, we believe that our results provide some useful indications.

In the oceans, the present performance of the global operational meteorological model at ECMWF, together with our results, suggest that a further increase of the resolution of the meteorological model will indeed bring the general results very close to the measured data. The maximum values are still a problem. In this respect, the model resolution and the horizontal diffusion introduced for numerical stability are obvious limiting factors. Our results indicate a substantial improvement with resolution, but they do not show the asymptotic behaviour that could suggest we are approaching the correct values. Many of the peaks have very reduced dimensions and are characterised by strong horizontal gradients. Even a T799 resolution, with the theoretical capability of identifying features of the order of 50 km or more, has obvious limitations. Note that in our experiments the physics of the model does not depend on resolution, with the exception of the horizontal diffusion, decreasing for increasing T values.

The wave results follow accordingly, with an expected enhancement due to the sensitivity to small wind variations. This is less the case for the maxima, because of their integral properties with respect to the driving wind fields. The wave bias found also at T799 is disappointing. However, a possible explanation is associated with the positions of the buoys. We have seen in Section 4 that the distributions of wind and wave biases in the Mediterranean Sea are not uniform. The highest values are found in the northern part of the basin, where the storms come from and the wind often blows from the coast towards the sea. There is evidence (Cavaleri and Bertotti, 2004) that in such cases the wind speed is underestimated, the bias decreasing while the wind propagates on the sea. The scale of the process, as derived from Fig. 5, is of the order of a few hundreds kilometres. Carrying out this analysis for different resolutions and different meteorological conditions suggests that the scale decreases with increasing resolution. Derived likely, but not exhaustive, reasons are the better description of the orography bordering the sea, a better definition of the coastline and the decreased diffusion, hence smoothing of the fields.

Independently of the reasons, the effect exists, and we expect different performances at buoys off the coast when the wind is coming from the open oceans or when the storm wind blows from the coast. In the latter case, if the buoys are sufficiently offshore the wind speed has already had enough time and space to reach or be close to the ‘correct’ values. Hence, the comparison between model and buoy measured values will show little or no bias. However, the local waves have been generated on the whole available fetch and carry with them the consequence of a wind speed underestimated along most of the fetch. In practice, the time and spatial scale required by modelled waves to reach the ‘correct’ values is larger than for wind speed. Therefore, on locations like the East coast of North America, where

the storms often blow from the West side, we should expect to find null or relatively small wind bias and a finite H_s bias. Indeed, checking the distribution of the biases among the different buoys, we have found this to be the case.

This explains also the results in the Mediterranean Sea and, more generally, in the enclosed seas. In practice, here the wind is always blowing from a coastline, and the effect becomes stronger the smaller the basin. Only where, like the north-west wind, Mistral, in the Western Mediterranean Sea, there is enough space available, the modelled wind speeds reach the ‘correct’ values. Then, as seen in Fig. 5, we find limited or no bias in the southern part of the basin, close to the African coast. On the contrary the wave heights, because of their integral properties over the generating wind field, will still show a substantial bias.

The hindcast of a cyclone had the aim of checking how well this phenomenon will be represented by a further increase of resolution with respect to the present T511. In this sense, our results are disappointing, because we have not found any substantial trend towards the reported values. One obvious limitation is the horizontal resolution. The scale required for a proper representation of this kind of storm close to its centre is of the order of a few kilometres at most. Therefore, in this area and with the present computer power, there is no possibility that a global model can accomplish this task. However, the lack of a tendency towards substantially higher (U_{10}) and lower (p) values when increasing the resolution may suggest that there is something else to be considered. Apart from the necessary parameterisation of the sub-grid processes, there have been arguments about the relevant physics in these extreme conditions. The possibility exists that the present formulation of the meteorological models does not include the necessary physics. This argument may also apply to the extremes in the extra-tropical storms.

7. Summary

In the oceans,

- a further increase of resolution will indeed bring the general results very close to the measured data, with errors expected to be between 1 and 2% for both wind speed and wave height,
- in the range of extreme values, there is still ample margin for improvement. While we see that increasing the resolution of the meteorological model does enhance the extreme values, both the trend with resolution and the comparison with data suggest further improvements are still necessary. It is suggested this may not depend only on the resolution, but also in an incorrect representation of the physics of the processes. The problem is more manifest for the wind speeds than for the wave heights, because the latter do not depend only on the local wind conditions.

In the enclosed basins,

- the present underestimate of both the wind speeds and the wave heights is only partially solved by an increase of resolution of the meteorological model, at least within the range we have explored. The available results suggest a strong influence of the land on

- the marine surface wind fields, for distances of some hundreds of kilometres. This implies that the wave heights are negatively biased for longer distances,
- the failure to model peak values is similar to the oceans, somehow enhanced by possible orographic effects. However, the wave peak values are more dependent on the wind peak values than in the oceans, because of the more local generation in the enclosed basins.

Acknowledgements

All the experiments discussed in this paper have been performed at the European Centre for Medium-Range Weather Forecasts, Reading, UK. We gratefully acknowledge the help of many members of the local staff in solving the unavoidable problems. In particular, we wish to thank Anthony Hollingsworth and Peter Janssen for their helpful discussions, and Niels Wedi and Jean Bidlot for guiding us through the intricacies of the numerical set-up. Jean Bidlot has also provided the wave data for the oceans.

John Ewing has done a careful review of the manuscript and provided useful comments.

References

- Abdalla, S., Cavaleri, L., 2002. Effect of wind variability and variable air density on wave modelling. *J. Geophys. Res.* 107 (C7), 17 (10.1029/2000JC000639).
- Bidlot, J.-R., Homes, D.J., Wittmann, P.A., Lalbeharry, R., Chen, H.S., 2002. Intercomparison of the performance of operational wave forecasting systems with buoy data. *Weather Forecasting* 17, 287–310.
- Cavaleri, L., Bertotti, L., 2003. The characteristics of wind and wave fields modelled with different resolutions. *Q. J. R. Meteorol. Soc.* 129, 1647–1662.
- Cavaleri, L., Bertotti, L., 2004. Accuracy of the modelled wind and wave fields in enclosed seas. *Tellus* 56A, 167–175.
- Cavaleri, L., Bertotti, L., Hortal, M., Miller, M., 1997. Effect of reduced diffusion on surface wind and wave fields. *Mon. Weather Rev.* 125 (11), 3024–3029.
- Komen, G.J., Cavaleri, L., Donelan, M., Hasselmann, K., Hasselmann, S., Janssen, P.A.E.M., 1994. *Dynamics and Modelling of Ocean Waves*. Cambridge University Press, New York, pp. 532.
- Powell, M.O., Vickery, P.J., Reinhold, T.A., 2003. Reduced drag coefficient for high wind speeds in tropical cyclones. *Nature* 422 (20), 279–283.
- Simmons, A., 1991. Development of the operational 31-level T213 version of the ECMWF forecast model. *ECMWF Newsllett.* 56, 3–13.
- Simmons, A., Hollingsworth, A., 2002. Some aspects of the improvement in skill of numerical weather prediction. *Q. J. R. Meteor. Soc.* 128, 647–677.
- Simmons, A., Mureau, R., Petroliaigis, T., 1995. Error growth and predictability estimates for the ECMWF forecasting system. *Q. J. R. Meteor. Soc.* 121, 1739–1771.